

10A.1

THE ROLE OF CONVEYOR BELTS IN ORGANIZING PROCESSES ASSOCIATED WITH HEAVY BANDED SNOWFALL

James T. Moore*, Sam Ng, and Charles E. Graves
Saint Louis University
St. Louis, Missouri

1. INTRODUCTION

Recent research on bands of heavy snowfall accompanying cyclogenesis has identified several key processes which synergistically interact to focus moisture, lift, and instability over mesoscale spatial and temporal scales. Numerous authors (Moore and Blakely 1988; Martin 1998; Grumm and Nicosia 1997; Nicosia and Grumm 1999; Market and Cissell 2002; Banacos 2003; Schumacher 2003; Novak et al. 2004; Jurewicz and Evans 2004, and Moore et al. 2005) have focused upon the roles of the trough of warm air aloft (trowal), frontogenetical forcing, and the development of conditional symmetric instability (CSI) in creating a narrow region of intense precipitation. A common theme to these investigations is the relationship of the aforementioned processes/features to the three major conveyor belts observed in cyclogenetic events (see Fig. 1). Recent numerical simulations clearly reveal that the three major conveyor belts play a critical role in deepening moisture within a favorable thermal profile for snow, developing instability, and enhancing mesoscale lift in a confined region northwest of the extratropical cyclone (ETC).

The purpose of this paper is to illustrate that the major processes and features associated with heavy banded snowfall can be conceptually understood within the context of the three atmospheric conveyor belts. It will be shown that it is the horizontal and vertical juxtaposition of these thermodynamically-contrasting conveyor belts which leads to a well-defined, often elongated mesoscale region of heavy banded snowfall. Perhaps more importantly, recognizing how these three air streams cooperatively interact to form mesoscale snow bands can help forecasters anticipate their formation at least 12 h prior to the onset of heavy snow, thereby increasing the lead time of the forecast.

*Corresponding author address: James T. Moore, Saint Louis University, Dept. of Earth and Atmospheric Sciences, St. Louis, MO 63103; e-mail: moore@eas.slu.edu.

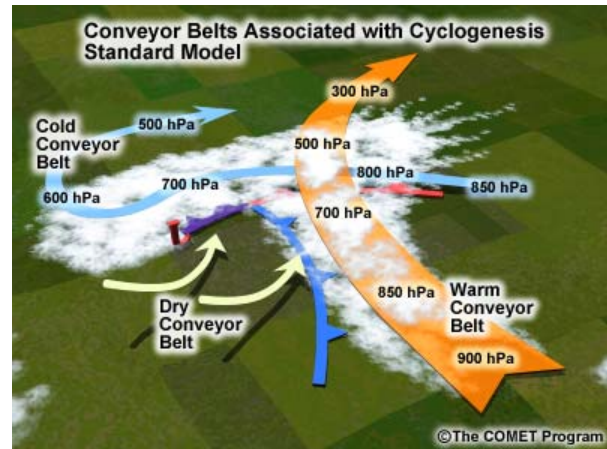


Figure 1. Standard view of atmospheric conveyor belts accompanying cyclogenesis (courtesy of the COMET program).

2. CONVEYOR BELTS

As noted by Moore et al. (2005), a conveyor belt can be envisioned as an ensemble of air parcels, originating from a common source region and layer, tracked over synoptic-scale time periods of 24-36 h. Typically, as noted by Browning (1990) and Carlson (1991), each air stream has unique thermodynamic characteristics, with relatively narrow ranges of potential temperature (θ ; for dry air) or equivalent/wet-bulb potential temperature (θ_e or θ_w ; for moist air). Conveyor belts can be hundreds of km wide and approximately 1-2 km in depth.

Atmospheric conveyor belts are best visualized through trajectories or system-relative flow in which the movement of the weather system (trough axis, absolute vorticity maximum, etc.) is subtracted from the wind field (Moore et al. 2005). The latter approach is best applied to weather systems that are not significantly weakening or strengthening with time and for which a representative system motion can be computed. Additionally, the system-relative wind field should only be used within the influence of the weather system being tracked. However, the use of atmospheric trajectories is less limiting and offers the user a more straight-forward interpretation

since cloud and precipitation systems are not developed instantaneously, but over spatial and temporal scales consistent with the path of air parcels traveling over synoptic-scale time periods.

Danielsen (1964) was the first researcher to use atmospheric trajectories to identify what later was termed the “dry conveyor belt” (DCB). He tracked mid-upper tropospheric air of high potential vorticity (PV) entering an ETC from the west-southwest. Typically, the visual manifestation of the DCB is a dry slot on water vapor satellite imagery, as schematically depicted in Fig. 1. However, recent numerical simulations and trajectory analysis have revealed that the DCB exhibits deformation as it approaches the ETC, thereby enhancing the cold/occluded frontal zones (Fig. 2). Also, the uppermost northern branch tends to turn cyclonically and ascend while the lowermost southern branch tends to turn anticyclonically while descending.

Harrold (1973) was the first to describe the warm conveyor belt (WCB). The WCB originates at low tropospheric levels (~950-850 hPa) within the warm sector of the ETC. In the warm sector it is typically associated with convective precipitation, but as it moves north of the warm front it tends to spread stratiform precipitation over a broad region. As depicted in Fig. 1 the WCB is often shown turning anticyclonically as it rises to the north, entering the mid-upper tropospheric westerlies. However, Martin (1998) noted that a branch of the WCB often turns cyclonically with height as it enters the ETC’s circulation, forming what Canadian meteorologist Penner (1955) termed the “trough of warm air aloft” or trowal airstream. Typically, one can identify the trowal as a ridge of high θ_e in the mid-troposphere (~700 hPa). Thus, the trowal branch of the WCB provides moisture and *synoptic-scale ascent* to the northwest side of the ETC. The bifurcation of the WCB typically occurs in the vicinity of the warm frontal zone (Fig. 2), thereby contributing to deformation and subsequent frontogenesis in this region of the ETC.

The cold conveyor belt (CCB) was first discussed in detail by Carlson (1980) as a system-relative airstream that approaches the ETC from the east, turning anticyclonically as it rises in the comma head (Fig. 1). However, Schultz (2001) has shown that at least one branch of the CCB turns cyclonically as it slowly rises, staying within the confines of the lower-troposphere. He proposed that there is a transition zone in the

comma head where the upper region of the CCB merges with the lower region of the WCB.

Thus, from recent research emerges a new picture of atmospheric conveyor belts which better describes the *four-dimensional* characteristics of these airstreams. Figure 2 reveals an updated picture of the three conveyor belts which attempts to illustrate the three-dimensional deformation processes attending these synoptic-scale flows. Trajectories derived from mesoscale numerical model simulations, along with an analysis of the trowal, frontogenesis, and regions of CSI, will be shown for two winter snowstorms to document the role of conveyor belts in forming the requisite mesoscale conditions required for heavy banded snow.

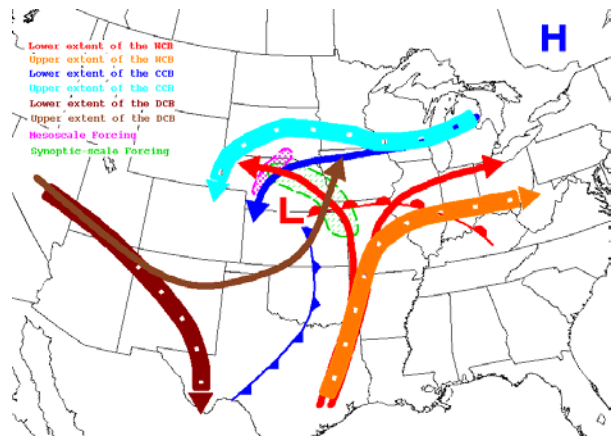


Figure 2. An updated schematic of conveyor belts illustrating their three-dimensional deformation characteristics (Ng 2005).

3. METHODS AND PROCEDURES

3.1 MM5 model simulations

Numerical simulations for the 26-27 November 2001 and 9-10 November 1998 winter storms were performed using the fifth generation Pennsylvania State University-National Center for Atmospheric Research Mesoscale Model (MM5; Dudhia et al. 2000). For each case a 48-h three-nest configuration with two-way interactions between domains was used. The three domains had grid spacings of 90 km, 30 km, and 10 km, respectively (Fig. 3). The largest grid was initialized at 1200 UTC 25 November 2001 and 0000 UTC 9 November 1998 for the two simulations, respectively. The MM5 model was initialized with the NCEP Eta 212 grid (40 km) model output every 12 h, which was acquired

through the National Center for Atmospheric Research (NCAR) Mass Storage System (MSS). The 30 km and 10 km grids were both initialized 6 h after the mother domain started its forward integration. Most of the results shown in this paper are from the 30 km grid. The 10 km grid was only used to display the precipitation estimates from the model. Parameterization schemes used in both simulations were identical for all three domains and included the following: Kain-Fritsch 2 for convective parameterization along with a shallow convection option, Goddard microphysics, Medium Range Forecast (MRF) planetary boundary layer, multi-layer soil diffusion, and CCM2 radiation scheme.

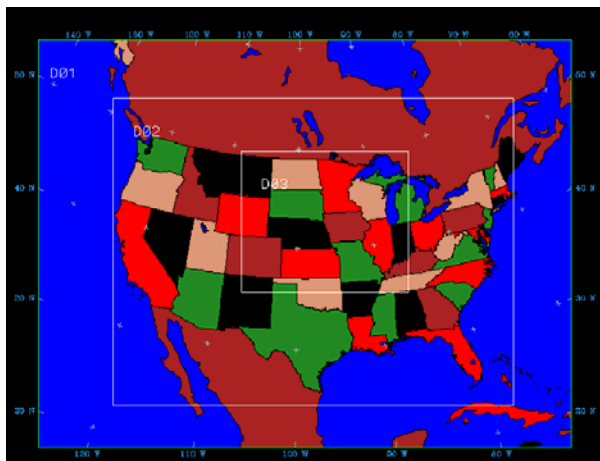


Figure 3. The three-domain (90, 30, and 10 km) nesting scheme used in the MM5 simulations of both winter storms; 26-27 November 2001 and 9-10 November 1998.

3.2 HYSPLIT Trajectories

The Hybrid Single-Particle Lagrangian Integrated Trajectory (HYSPLIT) model (Draxler and Hess 1998) was used to calculate trajectories within the CCB, WCB, and DCB. The HYSPLIT model used gridded data in the Air Resources Laboratory (ARL) format to compute trajectories onto a Lambert conformal map projection. Hourly MM5 model output was converted into the ARL format for proper data ingest. Both forward and backward dynamic trajectories can be run using u , v , and w components of the wind, temperature, height or pressure, moisture, and pressure at the surface from the model grid within an integrated advection scheme (see Draxler and Hess 1998 for details).

For both cases backward HYSPLIT trajectories were run 24 h from where the model

simulated the most intense precipitation. Nine backward trajectories were run equi-distant from each other at levels varying from 50 m to 5000 m AGL. By performing the backward trajectories first, a proper guess of the three major conveyor belts' source regions 24 h prior to the peak of the precipitation event could be obtained. Once possible starting locations were determined, a new matrix of trajectories were run going forward in time starting at 1800 UTC 25 November 2001 for the first case and 1200 UTC 9 November 1998 for the second case.

3.3 Pseudo Water Vapor Images

Pseudo water vapor images were generated from the MM5 model output by multiplying the ambient temperature ($^{\circ}\text{C}$) by the mixing ratio (q) and integrating the values over a 100-hPa layer from 500-400 hPa. In this way the mixing ratio effectively acts as a weighting function. From this method, a pseudo-brightness temperature (PBT) was calculated, where PBT values are negative at high altitudes since temperatures are less than 0°C in this region of the atmosphere. Small negative PBT values approaching zero correlate to a dry environment or warmer temperatures, while large negative PBT values are associated with a relatively moist layer or colder temperatures over the 500-400 hPa layer. A gray scale color-filled scheme is then applied from the PBT values to produce the pseudo water vapor images.

3.4 Equivalent Potential Vorticity

To diagnose regions of weak symmetric stability (WSS) or CSI equivalent potential vorticity (EPV) was computed using the three-dimensional form derived by McCann (1995). Since CSI is released in regions of lift and near-saturation the form of EPV used in the current research used θ_e instead of θ_{es} in regions of relative humidity greater than 80%. Values of EPV less than zero indicate regions of CSI or convective instability. However, operational research indicates that even regions where EPV is less than 0.25 PVU can be associated with banded precipitation (Schumacher 2003).

4. RESULTS

In this section results from both model simulations will be shown, with an emphasis on how the three major conveyor belts were intricately linked to the development of a region of

CSI, a zone of frontogenesis, and the formation of a trowal.

4.1 26-27 November 2001 Case

The 26-27 November 2001 snowstorm was associated with a cyclone that developed to the lee of the Rocky Mountains in Colorado and tracked through northwest Kansas, into Nebraska and western Iowa. This ETC was a relatively modest occluding cyclone with a central pressure only reaching a minimum of about 998 hPa. As occurs with many ETCs of this type, heavy snowfall fell mainly to the northwest of the occluding low. Actual 48-h snowfall amounts observed from the National Climatic Data Center revealed several bands of snowfall exceeding 10 inches in northwest Nebraska, north-central Nebraska, and southwest Minnesota, with the latter two areas receiving in excess of 20 inches! The MM5 model-simulated precipitation (Fig. 4) did relatively well in placing the heaviest precipitation amounts in Nebraska and Minnesota. The apparent model bias was to place the precipitation southeast of the observed location. However, a statistical correlation analysis revealed that the main model features (e.g., surface fronts, 850 hPa heights and moisture, 500 hPa height and vorticity, and 300 heights and winds) were highly correlated with the observed gridded data (not shown). Thus, the authors are confident that the basic physics of this event were captured by the model simulation. Therefore, in the following discussion we will compare the model forcing of the trowal, frontogenesis, and CSI to the model-generated precipitation.

For brevity, our discussion will focus upon the 21-h model forecast valid at 1500 UTC 26 November 2001, which is close to the time of maximum intensity of the precipitation. At this time a well-defined trowal axis at 700 hPa can be seen from Arkansas northward to Iowa where it begins its cyclonic turn to the northwest (Fig. 5). System-relative streamlines, which approximate trajectories, computed by subtracting the motion of the circulation center from the wind field, reveal excellent agreement with the distribution of the θ_e isentropes. While sloped isentropic ascent along the trowal axis provides synoptic-scale lift for air parcels entering the zone of precipitation, the advection of high θ_e also brings warm, moist air aloft to the northwest of the cyclone. Meanwhile, a

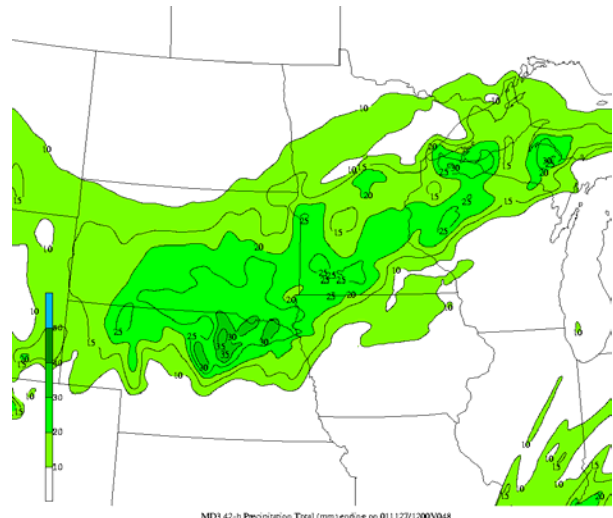


Figure 4. 10 km model simulated liquid precipitation (mm) for the 42 h period ending 1200 UTC 27 November 2001, beginning with the 10 mm contour. Note that 25 mm is ~10 inches of snow.

surge of dry air, seen as a dry slot on the pseudo water vapor imagery (Fig. 6), is entering western Iowa at this time. As will be seen shortly in the trajectory analysis, this dry slot is associated with the DCB which ascends into the ETC from the southwest. Nicosia and Grumm (1999) noted that when the DCB overlays moist air below, the EPV is reduced over a mesoscale region. In their case the moist air below the DCB was associated with the CCB. However, in the present case for the Midwest, it is far more common for the moist air below the DCB to be associated with the WCB.

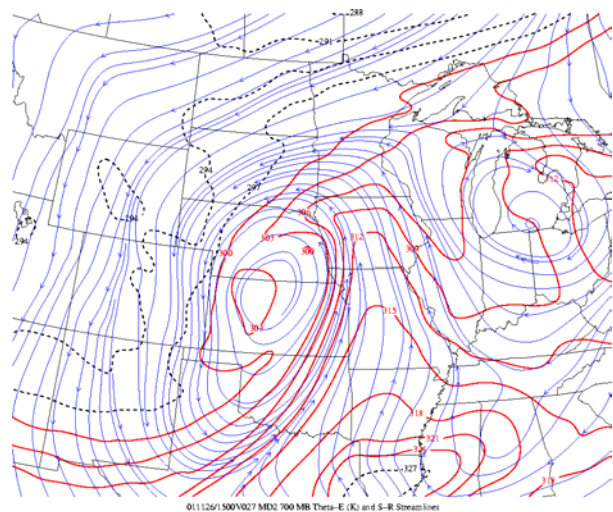


Figure 5. 30 km 21-h forecast of 700 hPa θ_e and system-relative streamlines valid at 1500 UTC 26 November 2001.

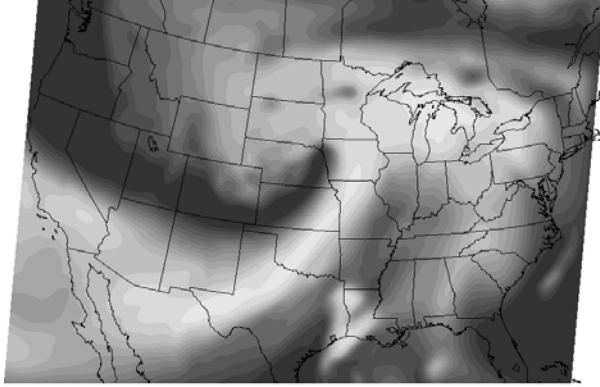


Figure 6. 30 km 21-h forecast of 500-400 hPa layer averaged pseudo water vapor imagery valid at 1500 UTC 26 November 2001.

If one superimposes the dry air from the west associated with the DCB over the warm moist air below associated with the trowal airstream, the EPV reduction zone forms over western Iowa. This is captured in Fig. 7, which displays both relative humidity and EPV over the region of interest. Note that values of EPV < 0.25 PVU are found along a zone on the eastern periphery of the dry slot seen in Fig. 6. Also, the most unstable air (EPV < 0 PVU) is found in a narrow region in western Iowa.

It is important to also note that the heaviest precipitation formed to the northwest of the EPV reduction zone where the greatest ascent was taking place. The reason for this mesoscale ascent can be found in the mid-tropospheric frontogenesis pattern seen in Fig. 8. The strongest mesoscale ascent typically is found on the equatorward side of the maximum frontogenetical forcing, placing it within the region of greatest model-generated precipitation (Fig. 4). Thus, the MM5 precipitation was located to the northwest of the trowal axis and most negative EPV and south of the strongest frontogenetical forcing, matching the conceptual models proposed by Moore et al. (2005) and Novak et al. (2004).

Figure 9 illustrates the HYSPLIT trajectories starting at 500 m AGL over eastern Texas. This lower extension of the WCB displays a cyclonic turn to the northwest, paralleling the system-relative streamlines shown in Fig. 5. However, Fig. 10 shows that when the same parcels are run at 1250 m AGL they take an anticyclonic turn to the northeast. Taken together, Figs. 9 and 10 show how the WCB undergoes a three - dimensional deformation as it moves

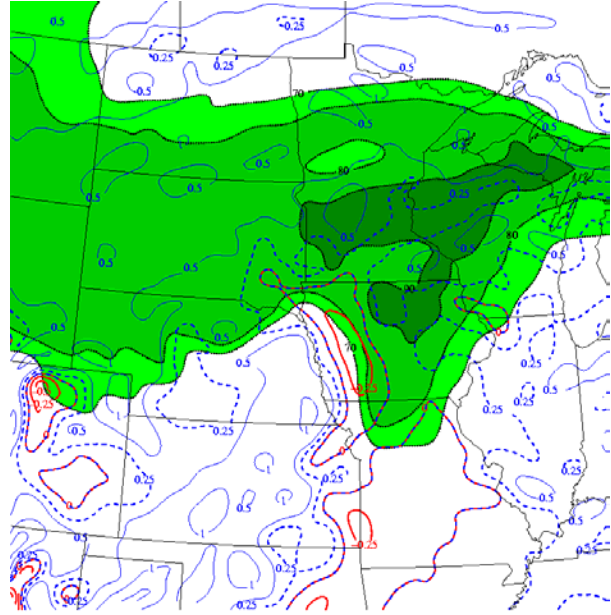


Figure 7. 30 km 21-h forecast of 700-500 hPa averaged EPV (alternating blue and red solid; EPV=0, red solid: EPV < 0.25 PVU, blue dashed: EPV = 0.25 PVU, and blue solid: EPV > 0.50 PVU; 1 PVU $1 \times 10^{-6} \text{ m}^2 \text{ s}^{-1} \text{ K kg}^{-1}$) and relative humidity > 70% shaded in green, valid at 1500 UTC 26 November 2001.

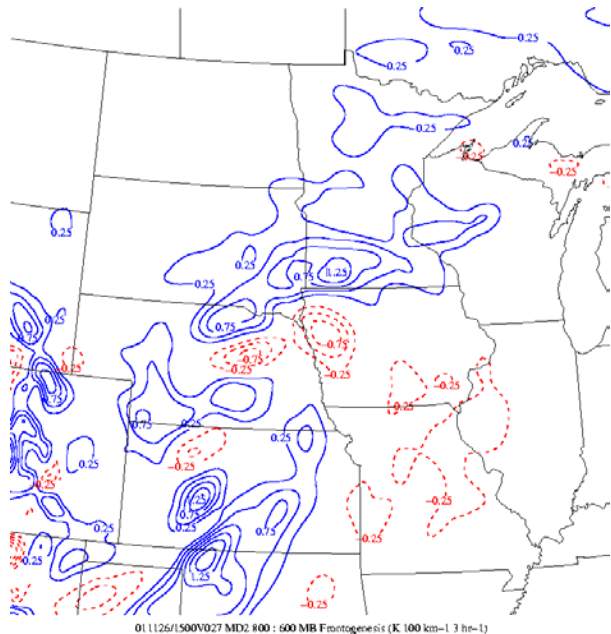


Figure 8. 30 km 21-h forecast of 800-600 hPa layer-averaged frontogenesis ($\text{K } 100 \text{ km}^{-1} \text{ 3 h}^{-1}$) valid at 1500 UTC 26 November 2001. Blue lines represent values > 0 and red dashed lines depict values < 0.

NATIONAL OCEANIC ATMOSPHERIC ADMINISTRATION
 Forward trajectories starting at 18 UTC 25 Nov 01
 12 UTC 25 Nov MM5 Forecast Initialization

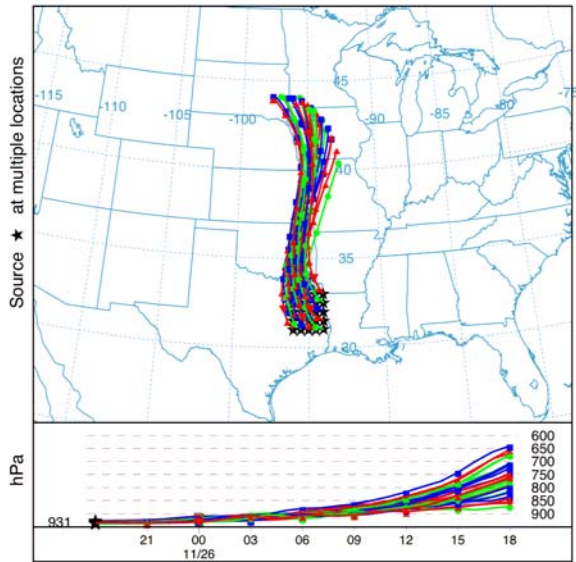


Figure 9. HYSPLIT 24-h forward trajectories over eastern Texas starting at 500 m AGL beginning 1800 UTC 25 November 2001.

NATIONAL OCEANIC ATMOSPHERIC ADMINISTRATION
 Forward trajectories starting at 18 UTC 25 Nov 01
 12 UTC 25 Nov MM5 Forecast Initialization

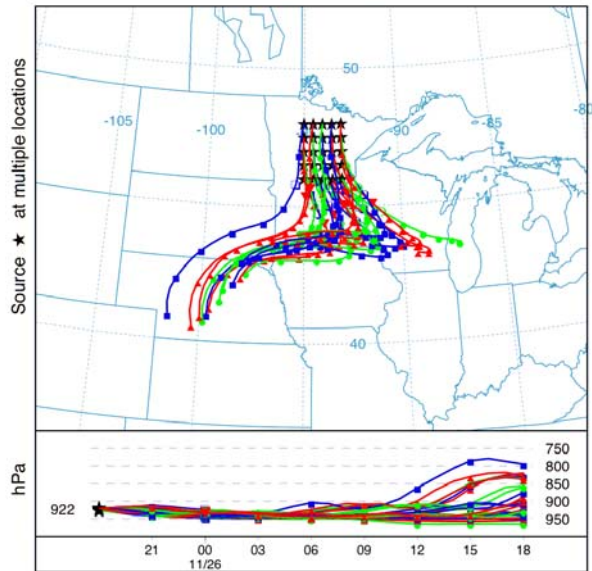


Figure 11. HYSPLIT 24-h forward trajectories over north-central Minnesota starting at 250 m AGL beginning 1800 UTC 25 November 2001.

NATIONAL OCEANIC ATMOSPHERIC ADMINISTRATION
 Forward trajectories starting at 18 UTC 25 Nov 01
 12 UTC 25 Nov MM5 Forecast Initialization

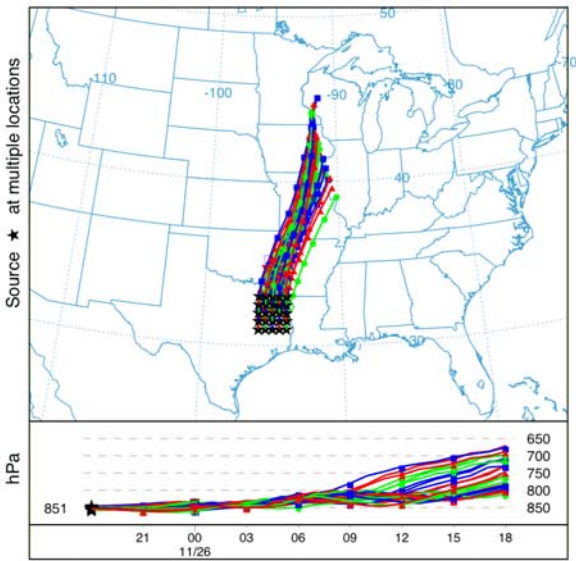


Figure 10. HYSPLIT 24-h forward trajectories over eastern Texas starting at 1250 m AGL beginning 1800 UTC 25 November 2001.

NATIONAL OCEANIC ATMOSPHERIC ADMINISTRATION
 Forward trajectories starting at 18 UTC 25 Nov 01
 12 UTC 25 Nov MM5 Forecast Initialization

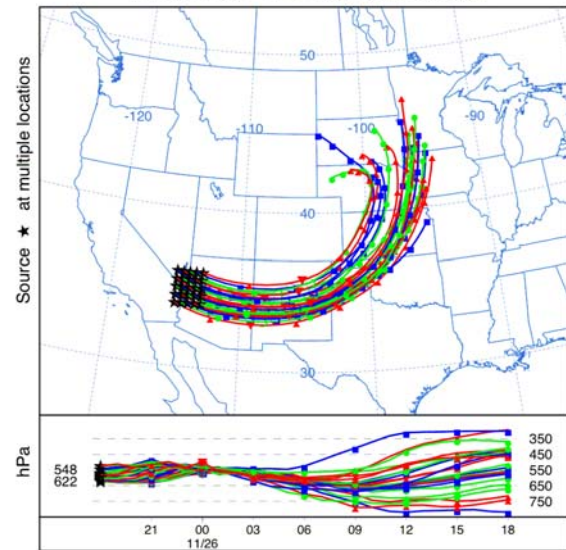


Figure 12. HYSPLIT 24-h forward trajectories over the border of Arizona, Nevada, and California starting at 3500 m AGL beginning 1800 UTC 25 November 2001.

northward. Generally, as air parcels are run at higher levels or at points further east, they tend to turn anticyclonically. *While it is the lower, westernmost air parcels that participate in the formation of the trowal airstream.*

From the backward trajectories, low-level air parcels were seen to be coming from north-central Minnesota associated with a cold anticyclone to the north. In Fig. 11 one sees that the CCB parcels move southward from Minnesota and turn cyclonically around the ETC while rising about 100 hPa during the 24-h period. Parcels run at higher levels AGL displayed more of a tendency to move to the south and east with time. The primary role of the CCB in this case appears to be that of supplying cold air in lower tropospheric levels to increase the low-level frontogenesis while keeping the air cold enough for snow to reach the ground.

Figure 12 shows those trajectories which best illustrate the DCB as parcels leave a matrix of locations over southern California, western Arizona, southern Nevada and move cyclonically to the northeast paralleling the dry slot illustrated earlier in Fig. 6. Notice that these parcels are generally much higher than the WCB parcels shown in Fig. 9, dramatically illustrating how these two conveyor belts work to decrease EPV in eastern Nebraska and western Iowa. When parcels were run from lower levels (~2500 m AGL) from the same initiation points, they showed a propensity to descend and turn anticyclonically as they moved toward the east. Thus, the DCB also displays a three-dimensional deformation pattern as air parcels in its upper extent move cyclonically and ascend, while air parcels in its lower extent move anticyclonically and descend.

Finally, Fig. 13 shows two trajectories from each conveyor belt to illustrate how the WCB (red line) and DCB (yellow line) overlap in the vicinity of western Iowa to reduce the EPV. Also, it displays how the interaction of the WCB and the CCB (blue line) acts to increase the low-mid tropospheric frontogenesis over a narrow region from northern Nebraska to southern Minnesota, in good agreement with the frontogenetical region shown in Fig. 8.

4.2 9-10 November 1998 Case

In contrast to the previous case, the snowfall of 9-10 November 1998 was associated with a very strong ETC that moved from

NATIONAL OCEANIC ATMOSPHERIC ADMINISTRATION
Forward trajectories starting at 18 UTC 25 Nov 01
12 UTC 25 Nov MM5 Forecast Initialization

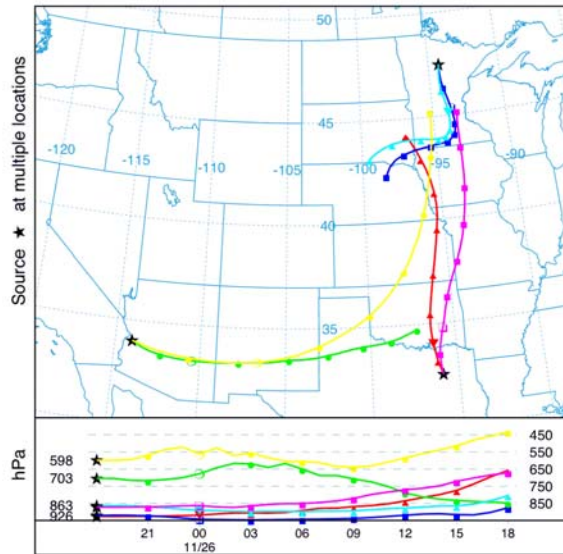


Figure 13. HYSPLIT 24-h forward trajectories over the major conveyor belt source regions at various heights beginning 1800 UTC 25 November 2001.

southeastern Colorado into central Kansas and northeastward into Minnesota. This occluding system eventually reached a central pressure of 964 hPa as it moved over Duluth, Minnesota in the late afternoon of 10 November. The MM5 model precipitation (Fig. 14) was located to the northwest

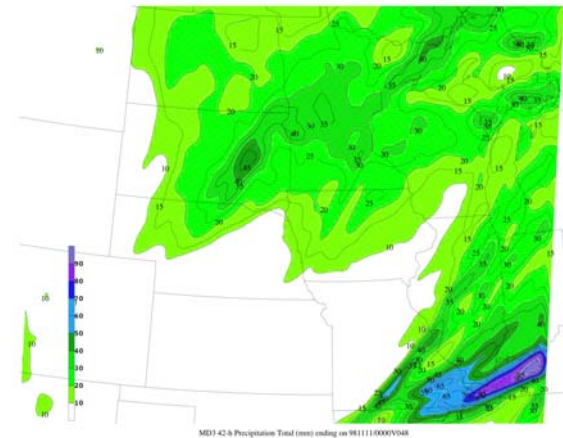


Figure 14. 10 km model simulated precipitation (mm) for the 42 h period ending 0000 UTC 11 November 1998, beginning with the 10 mm contour. Note that 25 mm is ~ 10 inches of snow.

of the actual heavy band of snow which fell over southeastern South Dakota. For more details concerning the synoptic situation for this case see Graves et al. (2003).

As in the first case, we will focus on 0900 UTC 10 November 1998, a few hours prior to the most intensive precipitation. The trowal axis at 700 hPa at 0900 UTC 10 November was located over the Mississippi and Ohio River valleys northwestward into eastern South Dakota (Fig. 15). The system-relative streamlines parallel the trowal axis, transporting warm, moist air to the northwest and west into South Dakota where the heaviest precipitation took place. Once again, the trowal is part of the lower branch of the WCB.

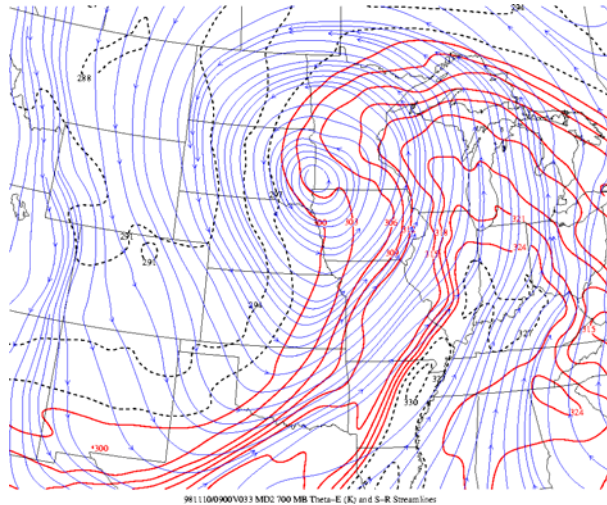


Figure 15. 30 km 27-h forecast of 700 hPa θ_e and system-relative streamlines valid at 0900 UTC 10 November 1998.

The dry slot in this case can be seen in the pseudo water vapor imagery (Fig. 16) as the dark area moving into southern Minnesota, with a second "punch" into Illinois. When one compares this image to Fig. 15, it is apparent that where the dry air overlays the warm, moist air of the trowal EPV is reduced. Thus, in Fig. 17 a large area of negative EPV is found from Missouri extending into a narrow tongue into south-central Minnesota. Another region of strongly negative EPV formed in central Illinois in response to the dry air moving into that region as well.

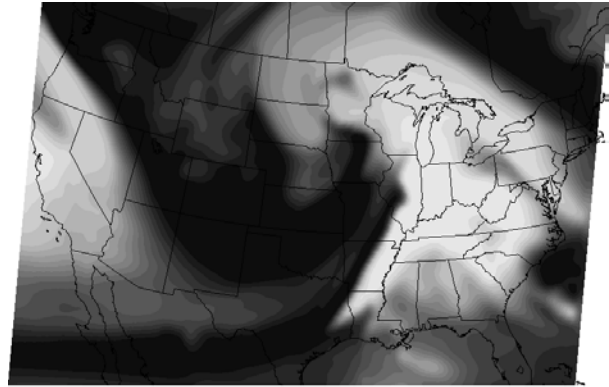


Figure 16. 30 km, 27-h forecast of 500-400 hPa layer averaged pseudo water vapor imagery valid at 0900 UTC 10 November 1998.

On the northwestern fringe of the trowal in northeastern South Dakota a mesoscale region of frontogenesis formed (Fig. 18). Referring to Fig. 14, one can see that the majority of the heavy precipitation fell to the southeast of the frontogen-

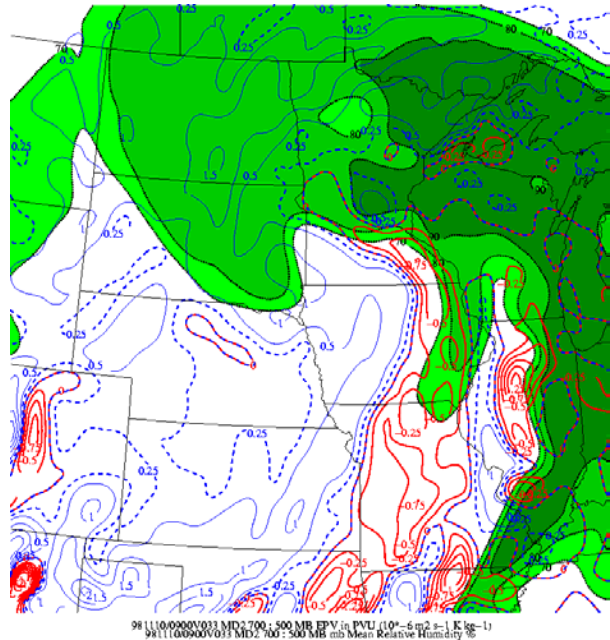


Figure 17. 30 km 27-h forecast of 700-500 hPa averaged EPV (alternating blue and red solid; EPV=0, red solid: EPV < 0.25 PVU, blue dashed: EPV = 0.25 PVU, and blue solid: EPV > 0.50 PVU; 1 PVU $1 \times 10^{-6} \text{ m}^2 \text{ s}^{-1} \text{ K kg}^{-1}$) and relative humidity > 70% shaded in green, valid at 0900 UTC 10 November 1998.

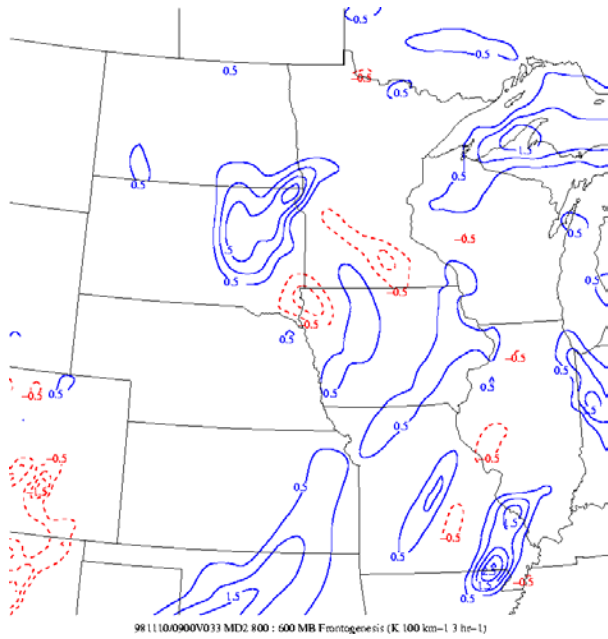


Figure 18. 30 km, 27-h forecast of 800-600 hPa layer averaged frontogenesis ($K 100 km^{-1} 3 h^{-1}$) valid at 0900 UTC 10 November 1998. Blue lines represent values > 0 and red dashed lines depict values < 0 .

NATIONAL OCEANIC ATMOSPHERIC ADMINISTRATION
Forward trajectories starting at 12 UTC 09 Nov 98
00 UTC 09 Nov MM5 Forecast Initialization

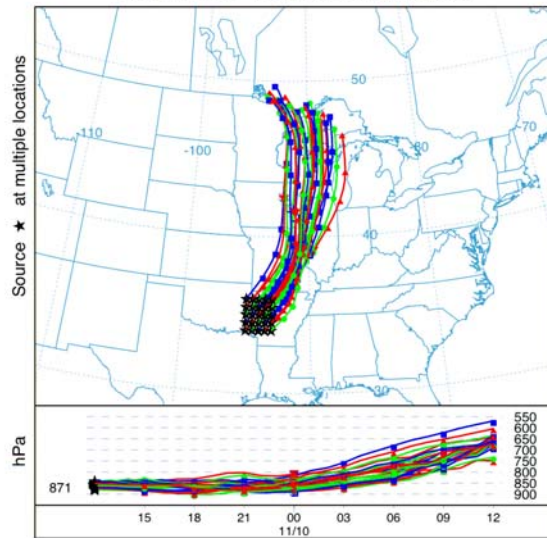


Figure 20. HYSPLIT 24-h forward trajectories over eastern Oklahoma and western Arkansas starting at 1000 m AGL beginning 1200 UTC 9 November 1998.

NATIONAL OCEANIC ATMOSPHERIC ADMINISTRATION
Forward trajectories starting at 12 UTC 09 Nov 98
00 UTC 09 Nov MM5 Forecast Initialization

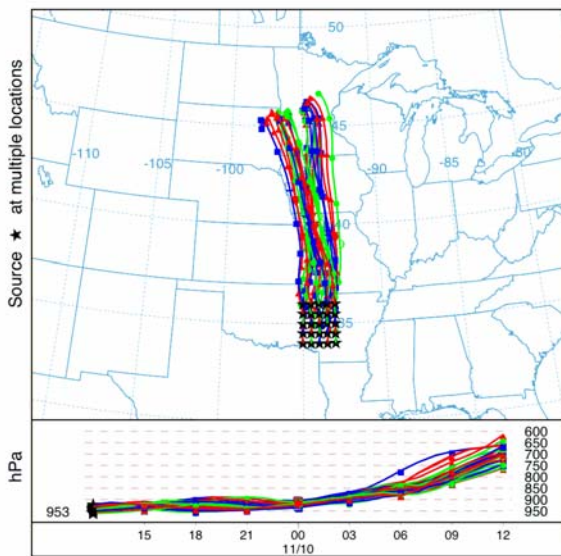


Figure 19. HYSPLIT 24-h forward trajectories over eastern Oklahoma and western Arkansas starting at 250 m AGL beginning 1200 UTC 9 November 1998.

NATIONAL OCEANIC ATMOSPHERIC ADMINISTRATION
Forward trajectories starting at 12 UTC 09 Nov 98
00 UTC 09 Nov MM5 Forecast Initialization

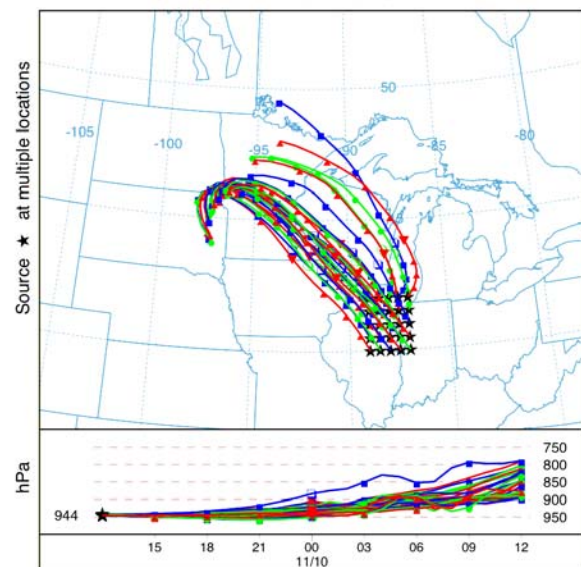


Figure 21. HYSPLIT 24-h forward trajectories over northeastern Illinois and northwestern Indiana starting at 250 m AGL beginning 1200 UTC 9 November 1998.

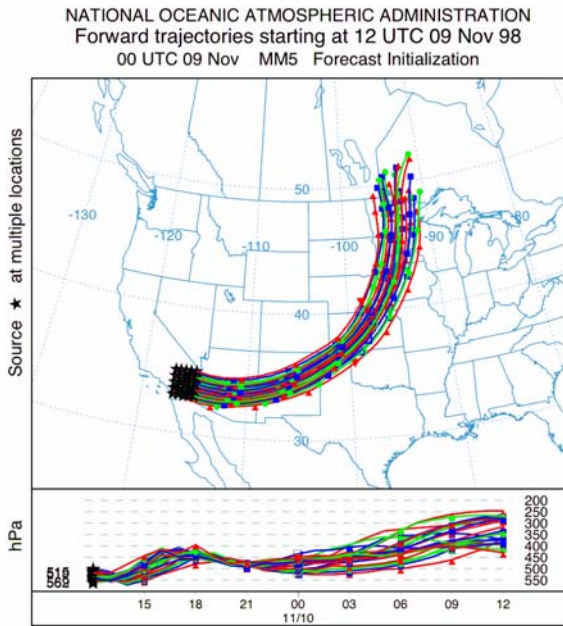


Figure 22. HYSPLIT 24-h forward trajectories over southern California starting at 4500 m AGL beginning 1200 UTC 9 November 1998.

sis axis. Thus, as noted in the first case, the most intense precipitation fell to the northwest of the trowal axis, in a region of weak symmetric stability, on the equatorward side of the frontogenesis maximum.

Figures 19 and 20 display the HYSPLIT trajectories representative of the WCB at 250 m and 1000 m AGL, respectively. As this ETC was strong, the lower and mid-tropospheric circulations were closed. Therefore, at both levels the trajectories are cyclonically curved, unlike the first case where the upper part of the WCB turned anticyclonically. Also, one can see that most of the vertical motion associated with the WCB's trowal airstream was focused within the last 6 h of the trajectory. This agrees with the time of greatest snowfall in southeastern South Dakota.

Figure 21 shows the paths of those parcels associated with the CCB. Parcels in this conveyor belt started in northeastern Illinois and northwestern Indiana and turned cyclonically as they entered the influence of the ETC near Minnesota and eastern South Dakota. However, these parcels did rise with time as they approached the circulation center. The CCB's initial location is very different from case one since the receding high pressure system was well east of the ETC during this time period. It appears that

once again, the role of the CCB was to maintain the supply of cold air to the northern reaches of the ETC, thereby maintaining a vertical temperature profile conducive to snow formation while also increasing the low-mid level frontogenesis in the region of interest.

The paths of the parcels associated with the DCB are illustrated in Fig. 22. The collective paths of these parcels correlate well with the dry slot shown in Fig. 16 that moved into Iowa and Minnesota. Comparing the WCB parcels shown in Fig. 19 and the DCB parcels shown in Fig. 22 demonstrates quite convincingly that the superposition of DCB with the WCB helped to reduce the EPV in Iowa and Minnesota.

Lastly, Fig. 23 depicts the trajectories of two parcels from each conveyor belt in one diagram to illustrate how they interacted to form an environment conducive to heavy snowfall. From this figure one can see how the DCB (yellow line) overlaps the WCB (red line) over western Iowa, thus documenting the EPV reduction process. Furthermore, it illustrates how the WCB (red line) brings warm, moist air northward in contact with cold air from the CCB (blue line). It should be noted that CCB parcels initialized at higher levels also turned cyclonically toward Minnesota and northern South Dakota, thereby contributing to low-mid tropospheric frontogenesis in Minnesota and northeastern South Dakota.

Figure 23 also demonstrates that there is a three-dimensional deformation process associated with both the WCB and DCB as they approach the cold front and warm front, respectively, associated with the occluding ETC. Note how the yellow (upper branch) and green (lower branch) trajectories of the DCB diverge both horizontally and vertically as they move eastward. Meanwhile, the red (lower branch) and magenta (upper branch) trajectories of the WCB both rise with time but diverge horizontally as they move north of the warm frontal zone associated with the ETC.

As with the first case, following the three major conveyor belts helps one to understand the development of frontogenetical zones, EPV reduction, and moisture advection in the region northwest of the ETC leading to heavy snowfall production.

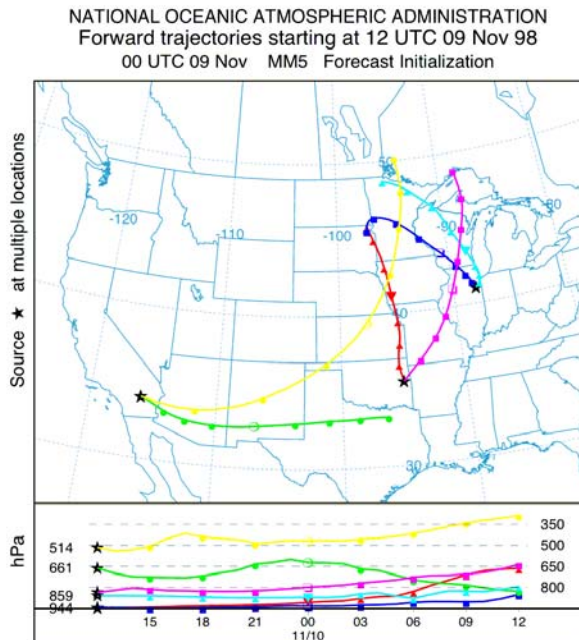


Figure 23. HYSPLIT 24-h forward trajectories over the major conveyor belt source regions at various heights beginning 1200 UTC 9 November 1998.

5. CONCLUSIONS

Two winter snowstorms, associated with heavy banded snowfall of greater than 10 inches in 24 h, were simulated using the MM5 model. Calculations of frontogenesis, EPV, system-relative streamlines, and a pseudo water vapor image helped document the critical processes associated with the banded precipitation. HYSPLIT trajectories were also run, based upon hourly model output, to illustrate the cold, dry, and warm conveyor belts. Several important conclusions from these two cases include:

- the lower branch of the WCB turns cyclonically and ascends, thereby forming the trowal airstream which brings warm, moist air to the northwest of the occluding cyclone,
- the upper branch of the WCB tends to turn anticyclonally as it ascends, joining the westerlies,
- the upper branch of the DCB turns cyclonically as it ascends into the ETC circulation,
- the upper branch of the DCB becomes superimposed over the warm, moist air of the WCB, resulting in an EPV reduction zone northwest of the trowal axis,
- the CCB remains at relatively low tropospheric levels as it slowly ascends into the ETC

circulation; it does **not** turn anticyclonally as it ascends,

- the CCB apparently helps to maintain a cold, low-tropospheric temperature profile conducive for snow while also interacting with the WCB to create a zone of frontogenesis northwest of the trowal axis, and
- the heaviest precipitation falls on the equatorward side of the frontogenesis axis, to the northwest of the trowal axis, and on the northern periphery of the region of minimum EPV.

In this way, the processes accompanying heavy banded snowfall can be understood in terms of the three major conveyor belts which are part and parcel of an ETC. Thus, it is the authors' contention that the preferred way to forecast heavy banded snowfall events is by 1) **recognizing the pattern** associated with these events, 2) **studying the magnitude and orientation of the ingredients** (e.g., frontogenesis, EPV, trowal, etc.) required for the snowfall, and 3) **understanding the processes** that are creating the banded nature of the snowfall. This is how the human forecaster can place a numerical model in the proper context to better conceptualize the physics playing out within the model atmosphere.

Acknowledgements. This work was supported by the NOAA Collaborative Science, Technology, and Applied Research (CSTAR) program under award NA03-NWS4680019. It is primarily derived from the second author's doctoral dissertation at Saint Louis University. We also would like to acknowledge the insight supplied by Dr. Greg Mann (SOO, Detroit/Pontiac NWS forecast office) and for serving on Dr. Ng's doctoral committee. The authors gratefully acknowledge the support of the UCAR Unidata program for supplying data for this project via the Internet Data Distribution (IDD) network and the Local Data Manager (LDM). Much of the software used for this research was also supplied by Unidata. We also would like to thank NCAR for permitting access to the Mass Storage System.

6. REFERENCES

Banacos, P.C., 2003: Short-range prediction of banded precipitation associated with deformation and frontogenetical forcing. *Preprints, 10th Conference on Mesoscale Processes*, Portland OR, Amer. Meteor. Soc.

- Browning, K.A., 1990: Organization of clouds and precipitation in extratropical cyclones. *Extratropical Cyclones-8, The Erik Palmen Memorial Volume*, C.W. Newton and E. O. Holopainen, Eds., Amer. Meteor. Soc., 129-153.
- Carlson, T.N., 1980: Airflow through midlatitude cyclones and the comma cloud pattern. *Mon. Wea. Rev.*, **108**, 1498-1509.
- Carlson, T.N., 1991: *Mid-Latitude Weather Systems*. Harper-Collins Academic, London, UK, 507 p.
- Danielsen, E.F., 1964: Project Springfield report. Tech. Rep. 1517, Defense Atomic Support Agency, HQ, Washington, D.C., 97 pp. [NTIS AD-607980].
- Draxler, R.R., and G. D. Hess, 1998: An overview of the HYSPLIT_4 modeling system for trajectories. *Aust. Met. Mag.*, **47**, 295-308.
- Dudhia, J., D. Gill, Y.-R. Guo, K. Manning, and W. Wang., 2000: PSU/NCAR mesoscale modeling system tutorial class notes and users guide: MM5 modeling system version 3. Tech. Rep., NCAR/MMM.
- Graves, C.G., J.T. Moore, M.J. Singer, and S. Ng, 2003: Band on the run - Chasing the physical processes associated with heavy snowfall. *Bull. Amer. Meteor. Soc.*, **84**, 990-994.
- Grumm, R.H. and D.J. Nicosia, 1997: WSR-88D Observations of mesoscale precipitation bands over Pennsylvania. *Nat. Wea. Dig.*, **21**, #3, 10-23.
- Harrold, T.W., 1973: Mechanisms influencing the distribution of precipitation within baroclinic disturbances. *Quart. J. Roy. Meteor. Soc.*, **99**, 232-251.
- Jurewicz, M. L., and M.S. Evans, 2004: A comparison of two banded, heavy snowstorms with very different synoptic settings. *Wea. Forecasting*, **19**, 1011-1028.
- Market, P.S. and D. Cissell, 2002: Formation of a sharp snow gradient in a Midwestern heavy snow event. *Wea. Forecasting*, **17**, 723-738.
- Martin, J.E., 1998: The structure and evolution of a continental winter cyclone. Part II: Frontal forcing of an extreme snow event. *Mon. Wea. Rev.* **126**, 329-348.
- McCann, D.W., 1995: Three-dimensional computations of equivalent potential vorticity. *Wea. Forecasting*, **10**, 798-802.
- Moore, J.T., and P.D. Blakely, 1988: The role of frontogenetical and conditional symmetric instability in the Midwest snowstorm of 30-31 January 1982. *Mon. Wea. Rev.*, **116**, 2155-2171.
- _____, C.E. Graves, S. Ng, and J.L. Smith, 2005: A process-oriented methodology towards understanding the organization of an extensive mesoscale snow band: A diagnostic case study of 4-5 December 1999. *Wea. Forecasting*, **20**, 35-50.
- Ng, S., 2005: *Development of a dynamical conceptual model of processes producing heavy banded snowfall utilizing numerical simulations*. Ph.D. dissertation, Saint Louis University, Department of Earth and Atmospheric Sciences, 342 p.
- Nicosia, D.J. and R.H. Grumm, 1999: Mesoscale band formation in three major northeastern United States snowstorms. *Wea. Forecasting*, **12**, 346-368.
- Novak, D.R., L.F. Bosart, D. Keyser, and J.S. Waldstreicher, 2004: An observational study of cold season banded precipitation in northeast U.S. cyclones. *Wea. Forecasting*, **19**, 993-1010.
- Penner, C.M, 1955: A three-front model for synoptic analyses. *Quart. J. Roy. Meteor. Soc.*, **81**, 89-91.
- Schultz, D.M. 2001: Reexamining the cold conveyor belt. *Mon. Wea. Rev.*, **129**, 2205-2225.
- Schumacher, P.N., 2003: An example of forecasting mesoscale bands in an operational environment. *Preprints, 10th Conference on Mesoscale Processes*, Portland, OR, Amer. Meteor. Soc.